Liquid Crystalline Bispropargyl Thermosets

David A. Langlois and Brian C. Benicewicz*

Polymers and Coatings Group, Los Alamos National Laboratory, Los Alamos, New Mexico 87545

Elliot P. Douglas

Department of Materials Science and Engineering, University of Florida, Gainesville, Florida 32611

Received February 13, 1998. Revised Manuscript Received July 13, 1998

A series of rigid-rod bispropargyl thermoset monomers have been synthesized. These monomers were examined by differential scanning calorimetry (DSC) and hot stage polarized optical microscopy. Enantiotropic or monotropic nematic liquid crystalline phases were observed for all but two monomers. Partial curing of these reactive liquid crystalline monomers resulted in the formation of stable liquid crystalline phases with broad nematic phase ranges. In one example, a monomer that was neither enantiotropic nor monotropic exhibited a stable nematic phase after partial curing. DSC investigations indicated that the onset temperature of thermally induced cross-linking was approximately 260 °C and insensitive to the phase type. The rate of cure was insensitive to the phase in which the cure occurred due to the unusual reaction mechanism for the propargyl end group.

Introduction

Investigations of liquid crystalline polymers have been largely motivated by their ability to exhibit a variety of interesting and useful properties, including high strength, high modulus fibers, films, and moldings, excellent barrier properties, and novel optical properties.[1−6] Over the last several years, interest in liquid crystalline thermosets (LCTs) has increased with the desire to improve the mechanical and physical properties of matrix materials for composite applications. Potential processing advantages may also exist with these new materials.[7,8]

The concept of LCTs has been described previously.[9−11] A liquid crystalline thermoset generally consists of a central mesogenic core end-capped with functional groups capable of reacting to provide a cross-linked network. It has now been widely shown that cross-linking can occur in the liquid crystalline phase to give a cross-linked network that retains the order of the liquid crystalline phase in the final solid form.

Propargyl-terminated resins have been proposed and evaluated as matrices for advanced polymeric composites.[12−14] They have been described as hydrophobic replacements for epoxies, possessing good thermal stability, low water absorption, good dielectric properties, low monomer sensitivity to boiling water, good solvent resistance, and excellent physical−mechanical properties. Their cure chemistry has been investigated and a mechanism has been described for the curing reactions. It was reported that curing of arylpropargyl ethers involves an initial rearrangement to a chromene (i.e., 2*H*-1-benzopyran) ring, which subsequently polymerizes via an ene−ene reaction.[15,16]

Previous reports from our laboratory and others have described an increasing variety of cross-linking groups that can be used in LCTs and reacted without interfering with the liquid crystalline order, including acrylates and methacrylates,[9−19] epoxies,[20−25] maleimides,[10,11]

* Present address of corresponding author: Department of Chemistry and Center for Polymer Synthesis, Rensselaer Polytechnic Institute, Troy, NY 12180.

(1) Ciferri, A.; Krigbaum, W. R.; Meyer, R. B. *Polymer Liquid Crystals*; Academic Press: New York, 1982.
(2) Ciferri, A. *Liquid Crystallinity in Polymers: Principles and Fundamental Properties*; VCH Publishers: New York, 1991.
(3) Chiou, J. S.; Paul, D. R. *J. Polym. Sci., Polym. Phys. Ed* **1987**, *25*, 1699.
(4) Weinkauf, D. H.; Paul, D. R. *J. Polym. Sci., Polym. Phys. Ed* **1991**, *29*, 329.
(5) Cantrell, G. R.; Freeman, H. B.; Hopfenberg, H. B.; Makhija, S.; Haider, I.; Jaffe, M. In *Liquid Crystalline Polymers*; Carfagna, C., Ed.; Pergamon Press: New York, 1993; p 233.
(6) Hikmet, R. A. M.; Lub, J.; Higgins, J. A. *Polymer* **1993**, *34*, 1736.
(7) Melissaris, A. P.; Litt, M. H. *Macromolecules* **1994**, *27*, 2675.
(8) Douglas, E. P.; Langlois, D. A.; Benicewicz, B. C. *Chem. Mater.* **1994**, *6*, 1925.
(9) Clough, S. B.; Blumstein, A.; Hsu, E. C. *Macromolecules* **1976**, *9*, 123.
(10) Hoyt, A. E.; Benicewicz, B. C. *J. Polym. Sci., Part A: Polym. Chem.* **1990**, *28*, 3403.
(11) Hoyt, A. E.; Benicewicz, B. C. *J. Polym. Sci., Part A: Polym. Chem.* **1990**, *28*, 3417.
(12) Dirlikov, S. K. *High Perform. Polym.* **1990**, *2*, 67.
(13) Douglas, W. E.; Overend, A. S. *Eur. Polym. J.* **1991**, *27*, 1279.
(14) Douglas, W. E.; Overend, A. S. *J. Mater. Chem.* **1993**, *3*, 27.
(15) Dirlikov, S. K.; Feng, Y. *Polym. Prepr.* **1991**, *32* (1), 363.
(16) Grenier-Loustalot, M. F.; Sanglar, C. *High Perform. Polym.* **1996**, *8*, 341.
(17) Broer, D. J.; Boven, J.; Mol, G. N. *Makromol. Chem.* **1989**, *190*, 2255.
(18) Broer, D. J.; Hikmet, R. A. M.; Challa, G. *Makromol. Chem.* **1989**, *190*, 3201.
(19) Litt, M. H.; Whang, W.-T.; Yen, K.-T.; Qian, X.-J. *J. Polym. Sci., Part A: Polym. Chem.* **1993**, *31*, 183.
(20) Barclay, G. G.; McNamee, S. G.; Ober, C. K. *Polym. Mater. Sci. Eng.* **1990**, *63*, 356.
(21) Barclay, G. G.; McNamee, S. G.; Ober, C. K. *Polym. Mater. Sci. Eng.* **1990**, *63*, 387.
(22) Rozenberg, B. A.; Gur'eva, L. L. *Polym. Mater. Sci. Eng.* **1992**, *66*, 162.

10.1021/cm980087b CCC: $15.00
Published on Web 09/25/1998

nadimides,[10,11] and acetylenes.[7,8] In this paper we describe our results relating the cure reaction and liquid crystallinity in new propargyl LCTs. Only one other publication in addition to our previous report has described propargyl LCTs.[26,27] However, where their interest was in developing cholesteric materials with unique optical textures, we have focused on understanding the phase behavior during cure.

Experimental Section

Synthesis. All diols were used as received except for 2-chlorohydroquinone, which was recrystallized from chloroform and then toluene and finally Soxhlet-extracted with hexane. All solvents and reagents were purchased from Aldrich Chemical Co. Dihydroxystilbene, dihydroxy-α-methylstilbene, and dihydroxy-2,2′-dimethylstilbene were synthesized according to reported literature procedures.[28,29] Elemental analysis was performed by Midwest Microlab, Indianapolis, IN.

Methyl-4-(propynyloxy)benzoate. Methyl-4-hydroxybenzoate (50.00 g, 0.329 mol) was dissolved in 250 mL of dimethylacetamide (DMAc). The solution was stirred as propargyl chloride (36.76 g, 0.493 mol) and potassium carbonate (68.14 g, 0.493 mol) were added. The brown slurry was then allowed to stir at 90 °C for 3 h. The reaction mixture was hot-filtered and 250 mL of water was added to the dark orange filtrate. The filtrate was cooled and filtered, isolating beige crystals that were dried at 30 °C in a vacuum. Yield 99%; mp 63 °C. The product was used without further purification but could be recrystallized from acetone/water. ^{1}H NMR (acetone-d_6): δ 7.97 (d, 2 H), 7.08 (d, 2 H), 4.88 (d, 2 H), 3.84 (s, 3 H), 3.12 (t, 1 H). ^{13}C NMR (acetone-d_6): δ 166.4, 162.2, 132.1, 124.1, 115.5, 79.0, 77.4, 56.6, 52.1.

4-(2-Propynyloxy)benzoic Acid. Sodium hydroxide (13.16 g, 0.329 mol) was dissolved in a solution of water (200 mL) and methanol (200 mL). Methyl-4-(propynyloxy)benzoate (50.00 g, 0.263 mol) was added with stirring and the orange solution was refluxed overnight. The solution was cooled to room temperature and acidified with concentrated HCl. The white product was isolated by filtration, washed with water, and dried at 80 °C overnight. Yield 97%, mp 215 °C. ^{1}H NMR (DMF-d_7): δ 8.00 (d, 2 H), 7.14 (d, 2 H), 4.97 (d, 2 H), 3.60 (t, 1 H). ^{13}C NMR (DMF-d_7): δ 167.6, 161.9, 132.1, 124.8, 115.3, 79.3, 78.2, 56.4.

4-(2-Propynyloxy)benzoyl Chloride. 4-(2-Propynyloxy)-benzoic acid (50.00 g, 0.284 mol) was suspended in benzene (300 mL) with stirring. Oxalyl chloride (90.12 g, 0.710 mol) was slowly added to the mixture (gas evolved). The mixture was slowly heated to reflux and allowed to reflux for 3 h. The excess oxalyl chloride and approximately 30% of the benzene were removed by distillation. The remaining dark red solution was cooled. To this was added hexane (300 mL), and the mixture was reheated to reflux and hot-filtered. Upon cooling, yellow-tan crystals were isolated by filtration and dried at 30 °C in a vacuum. Yield 76%, mp 63 °C. ^{1}H NMR ($CDCl_3$): δ 8.07 (d, 2 H), 7.03 (d, 2 H), 4.77 (d, 2 H), 2.56 (t, 1 H). ^{13}C NMR ($CDCl_3$): δ 167.0, 163.1, 133.8, 126.3, 115.1, 77.2, 76.6, 56.1.

Bispropargyl Monomer Synthesis. The bispropargyl monomers were synthesized by the same general procedure as described here for monomer **1**. Hydroquinone (1.25 g, 0.0114 mol), ether (30 mL), and triethylamine (2.31 g, 0.0228 mol) were allowed to stir in an ice bath for 0.5 h. 4-(2-Propynyloxy)benzoyl chloride (4.44 g, 0.0288 mol) was slowly added to the stirring mixture. The beige slurry was stirred at room temperature for 3 h. The ether was removed with a rotary evaporator and the remaining beige product was stirred in warm water (50 mL). A beige product was isolated by filtration and dried at 50 °C in a vacuum. The products were recrystallized from the appropriate solvents listed below and dried at 80 °C in a vacuum.

Monomer 1. Recrystallized from acetonitrile. ^{1}H NMR (DMSO-d_6): δ 8.11 (d, 4 H), 7.35 (s, 4 H), 7.18 (d, 4 H), 4.95 (d, 4 H), 3.64 (t, 2 H). ^{13}C NMR (DMSO-d_6): δ 164.1, 161.6, 148.0, 131.9, 122.9, 121.6, 115.1, 78.7, 78.5, 55.8. Anal. Calcd for $C_{26}H_{18}O_6$: C, 73.10; H, 4.25; O, 22.51. Found: C, 73.10; H, 4.22.

Monomer 2. Recrystallized from acetonitrile. ^{1}H NMR (DMSO-d_6): δ 8.11 (m, 4 H), 7.20 (m, 7 H), 4.95 (m, 4 H), 3.64 (m, 2 H), 2.17 (s, 3 H). ^{13}C NMR (DMSO-d_6): δ 164.1, 163.7, 161.6, 148.0, 146.7, 131.8, 131.3, 124.0, 123.0, 121.6, 121.4, 120.3, 115.1, 78.7, 78.5, 55.8, 15.7. Anal. Calcd for $C_{27}H_{20}O_6$: C, 73.63; H, 4.58; O, 21.79. Found: C, 73.42; H, 4.61.

Monomer 3. Recrystallized from acetonitrile. ^{1}H NMR (DMSO-d_6): δ 8.13 (d, 4 H), 7.18 (d, 4 H), 7.12 (s, 2 H), 4.95 (d, 4 H), 3.65 (t, 2 H), 2.09 (s, 6 H). ^{13}C NMR (DMSO-d_6): δ 163.9, 161.6, 146.6, 131.8, 130.2, 121.4, 120.2, 115.1, 78.7, 78.5, 55.8, 12.7. Anal. Calcd for $C_{28}H_{22}O_6$: C, 74.00; H, 4.88; O, 21.12. Found: C, 73.87; H, 4.97.

Monomer 4. Recrystallized from 2-propanol. ^{1}H NMR (DMSO-d_6): δ 8.10 (m, 4 H), 7.23 (d, 1H), 7.17 (m, 5 H), 6.89 (d, 1 H), 4.95 (m, 4 H), 3.75 (s, 3 H), 3.65 (t, 2 H). ^{13}C NMR (DMSO-d_6): δ 164.0, 163.5, 161.5, 151.5, 149.0, 137.0, 131.9, 123.1, 121.6, 121.4, 115.1, 113.7, 107.4, 78.7, 78.5, 56.1, 55.8. Anal. Calcd for $C_{27}H_{20}O_7$: C, 71.05; H, 4.42; O, 24.54. Found: C, 70.84; H, 4.45.

Monomer 5. Recrystallized from acetonitrile/DMF. ^{1}H NMR (DMSO-d_6): δ 8.13 (m, 4 H), 7.66 (d, 1 H), 7.54 (d, 1 H), 7.38 (m, 1 H), 7.18 (m, 4 H), 4.95 (m, 4 H), 3.63 (m, 2 H). ^{13}C NMR (DMSO-d_6): δ 163.8, 163.2, 161.9, 161.7, 148.6, 144.4, 132.0, 126.2, 124.8, 123.8, 122.1, 121.2, 120.7, 115.2, 78.7, 78.4, 55.8. Anal. Calcd for $C_{26}H_{17}ClO_6$: C, 67.76; H, 3.72; Cl, 7.69; O, 20.83. Found: C, 67.57; H, 3.69; Cl, 7.65.

Monomer 6. Recrystallized from acetonitrile. ^{1}H NMR (DMSO-d_6): δ 8.13 (d, 2 H), 7.97 (d, 2 H), 7.38 (m, 8 H), 7.15 (m, 4 H), 4.95 (m, 4 H), 3.63 (m, 2 H). ^{13}C NMR (DMSO-d_6): δ 163.9, 161.5, 148.4, 145.0, 136.0, 135.2, 131.8, 128.5, 128.3, 127.8, 124.4, 123.6, 122.0, 121.6, 121.3, 115.0, 78.7, 78.5, 55.8. Anal. Calcd for $C_{32}H_{22}O_6$: C, 76.48; H, 4.41; O, 19.10. Found: C, 76.20; H, 4.35.

Monomer 7. Recrystallized from DMF/H_2O. ^{1}H NMR (DMSO-d_6): δ 8.15 (d, 4 H), 8.03 (d, 2 H), 7.88 (s, 2 H), 7.50 (d, 2 H), 7.20 (d, 4 H), 4.96 (d, 4 H), 3.65 (t, 2 H). ^{13}C NMR (DMSO-d_6): δ 164.2, 161.6, 148.3, 131.9, 131.3, 128.9, 122.5, 121.6, 118.7, 115.1, 78.7, 78.5, 55.8. Anal. Calcd for $C_{30}H_{20}O_6$: C, 75.62; H, 4.23; O, 20.15. Found: C, 75.57; H, 4.30.

Monomer 8. Recrystallized from DMF/H_2O. ^{1}H NMR (DMSO-d_6): δ 8.12 (d, 4 H), 7.77 (d, 4 H), 7.36 (d, 4 H), 7.18 (d, 4 H), 4.95 (d, 4 H), 3.65 (t, 2 H). ^{13}C NMR (DMSO-d_6): δ 164.0, 161.5, 150.2, 136.9, 131.8, 127.7, 122.3, 121.6, 115.1, 78.7, 78.5, 55.8. Anal. Calcd for $C_{32}H_{22}O_6$: C, 76.48; H, 4.41; O, 19.10. Found: C, 76.36; H, 4.45.

Monomer 9. Recrystallized from acetonitrile. ^{1}H NMR (DMSO-d_6): δ 8.11 (d, 4 H), 7.19 (m, 10 H), 4.95 (d, 4 H), 3.64 (t, 2 H), 2.06 (s, 6 H). ^{13}C NMR (DMSO-d_6): δ 164.0, 161.5, 149.7, 137.7, 137.0, 131.8, 130.1, 122.9, 121.7, 119.1, 115.1, 78.7, 78.5, 55.8, 19.4. Anal. Calcd for $C_{34}H_{26}O_6$: C, 76.97; H, 4.94; O, 18.09. Found: C, 76.85; H, 5.04.

Monomer 10. Recrystallized from DMF/H_2O. ^{1}H NMR (DMSO-d_6): δ 8.10 (d, 4 H), 7.69 (d, 4 H), 7.22 (m, 10 H), 4.95 (d, 4 H), 3.65 (t, 2 H). ^{13}C NMR (DMSO-d_6): δ 164.0, 161.5, 150.0, 134.7, 131.8, 127.6, 127.4, 122.1, 121.6, 115.1, 78.7, 78.5, 55.8. Anal. Calcd for $C_{34}H_{24}O_6$: C, 77.26; H, 4.58; O, 18.16. Found: C, 77.16; H, 4.54.

(23) Mallon, J. J.; Adams, P. M. *J. Polym. Sci., Part A: Polym. Chem.* **1993**, *31*, 2249.
(24) Broer, D. J.; Lub, J.; Mol, G. N. *Macromolecules* **1993**, *26*, 1244.
(25) Jahromi, S.; Kuipers, W. A. G.; Norder, B.; Mijs, W. J. *Macromolecules* **1995**, *28*, 2201.
(26) Douglas, E. P.; Langlois, D. A.; Benicewicz, B. C. U.S. Patent 5,475,133, 1995.
(27) Kricheldorf, H. R.; Gerken, A. *High Perform. Polym.* **1997**, *9*, 75.
(28) Becker, K. B. *Synthesis* **1983**, 341.
(29) Zaheer, S. H.; Singh, B.; Bhushan, B.; Bhargava, P. M.; Kacker, I. K.; Ramachandran, K.; Sastri, V. D. N.; Rao, N. S. *J. Chem. Soc.* **1954**, 3360.

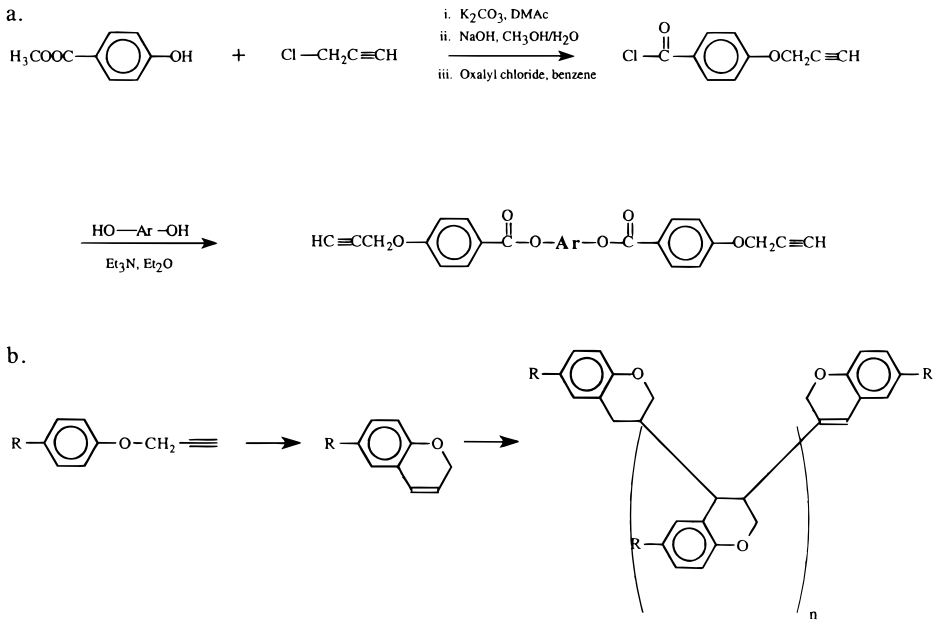

Figure 1. (a) Reaction scheme for the synthesis of bispropargyl thermosets and (b) intramolecular propargyl rearrangement followed by chromene polymerization.

Monomer 11. Recrystallized from acetonitrile/DMF. ^{1}H NMR (DMSO-d_6): δ 8.11 (d, 4 H), 7.67 (d, 2 H), 7.50 (d, 2 H), 7.29 (m, 4 H), 7.18 (d, 4 H), 6.96 (s, 1 H), 4.95 (d, 4 H), 3.65 (t, 2 H), 2.28 (d, 3 H). ^{13}C NMR (DMSO-d_6): δ 164.0, 161.5, 149.9, 149.1, 140.6, 135.9, 135.3, 131.8, 130.0, 126.8, 126.5, 121.7, 115.1, 78.7, 78.5, 55.8, 17.1. Anal. Calcd for $C_{35}H_{26}O_6$: C, 77.48; H, 4.83; O, 17.69. Found: C, 77.20; H, 4.82.

Monomer 12. Recrystallized from acetonitrile/DMF. ^{1}H NMR (DMSO-d_6): δ 8.13 (d, 4 H), 7.58 (s, 2 H), 7.49 (d, 2 H), 7.20 (m, 8 H), 4.95 (d, 4 H), 3.65 (t, 2 H), 2.18 (s, 6 H). ^{13}C NMR (DMSO-d_6): δ 163.7, 161.6, 148.7, 134.8, 131.8, 130.1, 128.7, 127.6, 125.1, 122.5, 121.5, 115.1, 78.7, 78.5, 55.8, 15.8. Anal. Calcd for $C_{36}H_{28}O_6$: C, 77.68; H, 5.07; O, 17.25. Found: C, 77.39; H, 5.33.

Thermal Analysis. Differential scanning calorimetry (DSC) was performed with a Polymer Laboratories DSC operated at heating rates of 10 or 20 °C/min, as indicated. Transition temperatures were reported as the extrapolated onset. Optical microscopy was performed with a Zeiss universal microscope equipped with a Linkam hot stage. Samples were placed between glass cover slips on the hot stage and observed between crossed polarizers at heating and cooling rates of 10 or 20 °C/min. Curing studies were performed with a Seiko Instruments DSC 220C. Samples were placed in a DSC sample pan and cured isothermally in an oven for various times. Partially cured samples were then heated at 20 °C/min in the DSC to determine the residual cure exotherm remaining after the isothermal cure. The fraction of uncured material remaining after the isothermal cure was then determined by $f = \Delta H_t/\Delta H_0$, where ΔH_t is the cure exotherm for the partially cured sample and ΔH_0 is the cure exotherm for the uncured sample.

Nuclear Magnetic Resonance Spectroscopy. NMR spectra were obtained with a Bruker AC250 250 MHz spectrometer using DMSO-d_7, acetone-d_6, DMF-d_7, or $CDCl_3$ as the solvent.

Results and Discussion

Synthesis. The synthetic scheme for the target monomers studied in this work is shown in Figure 1a. The synthesis involved the reaction of an end-capping reagent, 4-(2-propynyloxy)benzoyl chloride,[26,27] with a wide variety of diols performed under standard condensation conditions as described in the Experimental Section. This is the same general scheme that has been used previously to prepare LCTs with a wide variety of cross-linking end groups.[8,10,11,27] The end-capping reagent was synthesized by the reaction of propargyl chloride with methyl-4-hydroxybenzoate under Williamson ether synthesis conditions. The methyl ester thus obtained was hydrolyzed under basic conditions in aqueous methanol and converted to the acid chloride using oxalyl chloride. The end-capping reagent was synthesized at a sufficiently large scale to allow a library of compounds to be easily prepared, and subsequently studied, by reaction with common diols. The monomers synthesized in this study are shown in Table 1.

Microscopy Observations. All of the monomers were observed between crossed polarizers during heating, cooling, and at various stages of cure. The nematic phase was the only liquid crystalline phase observed throughout the study on these materials. A previous study has shown that chiral propargyl LCTs exhibit a cholesteric liquid crystalline phase.[27] Enantiotropic nematic phases were seen for most of the monomers in Table 1. Exceptions to this were the unsymmetrical methyl- and methoxy-substituted monomers **2** and **4**. These monomers displayed monotropic nematic phases. However, curing of these monomers at elevated temperatures produced materials with enantiotropic nematic phases and wide biphasic ranges.

To prepare for the curing measurements described below, we examined the phase behavior during isothermal cure for both monomers **1** and **5**. Phase behavior was observed up to the gel time during isothermal cure at 215, 230, 245, and 260 °C, which are the same temperatures used for the curing studies. Monomer **5** was isotropic at all temperatures. However, monomer **1** exhibited different phases, depending on the temperature. At 215 °C monomer **1** was nematic. At 230 °C monomer **1** was initially isotropic, but very rapidly a liquid crystalline phase formed and the cure was carried out in a biphasic structure consisting of coexisting nematic and isotropic domains. At 245 and 260 °C

Table 1. Structure and Phase Behavior of Bispropargyl Thermosets[a]

monomer	Ar	DSC (°C)	Exotherms (°C) Extrap. Onset	Peak Max.	Microscopy Observations
1		k $\xrightarrow{142}$ k_1 $\xrightarrow{167}$ lc $\xrightarrow{222}$ i	262	302	nematic
2	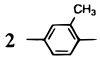	k $\xrightarrow{170}$ i	262	300	monotropic nematic
3	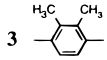	k $\xrightarrow{158}$ lc $\xrightarrow{196}$ i	263	301	nematic
4	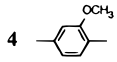	k $\xrightarrow{135}$ i	262	302	monotropic nematic
5	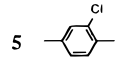	k $\xrightarrow{196}$ i	267	304	nematic after curing
6	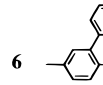	k $\xrightarrow{119}$ i	266	306	isotropic
7	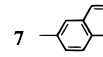	k $\xrightarrow{210}$ lc $\rightarrow$ exo	263	302	nematic
8	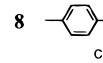	k $\xrightarrow{162}$ k_1 $\xrightarrow{187}$ lc $\rightarrow$ exo	263	298	nematic
9	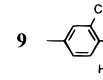	k $\xrightarrow{134}$ lc $\xrightarrow{211}$ i	269	303	nematic
10	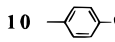	k $\xrightarrow{191}$ lc $\rightarrow$ exo	263	302	nematic
11	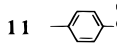	k $\xrightarrow{167}$ lc $\rightarrow$ exo	267	302	nematic
12	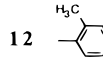	k $\xrightarrow{203}$ lc $\rightarrow$ exo	265	303	nematic

[a] DSC transitions are recorded as extrapolated onsets. k, crystal; lc, liquid crystal; i, isotropic liquid; exo, exotherm. Heating rate 20 °C/min.

monomer **1** was isotropic throughout the cure.

In our earlier work, a transformation diagram was proposed to describe the relationship between cure and liquid crystallinity in reactive LCTs.[11] This model attempted to explain the major features of the phase behavior of LCTs. The first feature was the depression of the solid to nematic transition temperatures upon partial curing or B-staging. This behavior was ascribed to the mixture of reaction products formed at the earlier stages of oligomerization, essentially a mixed melting point effect. The other major feature was the increase in the isotropization temperature and formation of a biphasic region that was a result of the chain extension occurring simultaneously with oligomerization. These two phenomena led to an increase in the liquid crystalline phase range upon curing. Experimental observation of all these phenomena in a single system was difficult in previously reported systems because of the high melting points of the monomers, the absence of an isotropization temperature below the decomposition temperature of the material, or the rapid rate of reaction characteristic of the end group at elevated temperatures. However, with the bispropargyl LCTs, it was possible to observe and verify these features in a single system. The experimentally determined transformation diagram for compound **1** is shown in Figure 2. Samples of monomer **1** were held at 200 °C for 30, 60, 90, and 120 min. After the sample was held for the designated time, it was heated at 10 °C/min and the temperature of the first appearance of isotropic droplets in the continuous nematic fluid was recorded and used to graph the lower nematic−isotropic phase boundary in Figure 2. Continued heating of the sample to complete isotropization determined the temperature for the upper nematic−isotropic phase boundary in Figure 2. After isotropization, the sample was cooled to verify the upper nematic−isotropization transition temperature, which

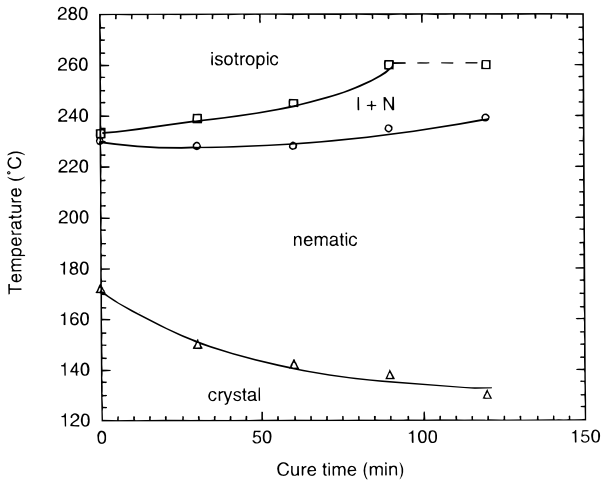

Figure 2. Experimentally determined transformation diagram for compound **1** cured at 200 °C. The dotted line indicates those samples that underwent cross-linking before isotropization.

Table 2. Transition Temperatures for Partially Cured Thermoset 1 Determined by Optical Microscopy[a]

cure time (min)	$k - n$ (°C)	initial isotropization (°C)	complete isotropization (°C)
30	150	228	239
60	142	228	245
90	138	235	>260
120	130	239	>260

[a] Cure temperature 200 °C.

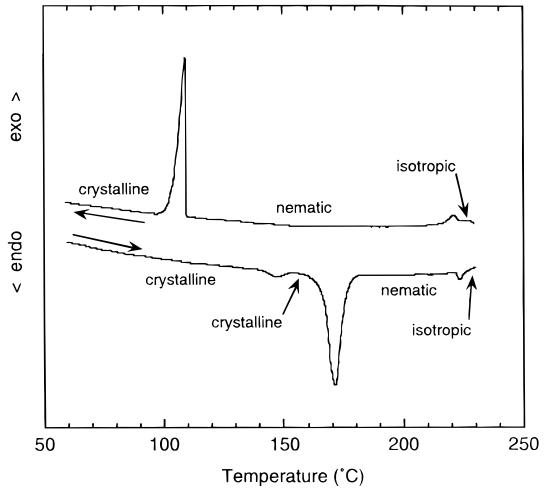

Figure 3. DSC heating and cooling curves for compound **1** recorded at 10 °C/min.

occurred sharply with the appearance of nematic droplets. Separate samples were often used to determine the crystal to nematic melting temperatures, especially when the previous heating experiments raised the temperature near the onset of rapid cross-linking. Thus, after holding the sample for the designated time and cooling to room temperature, the sample was reheated at 10 °C/min for determination of the crystal to nematic melting temperature. The data are provided in Table 2. At cure times of 90 and 120 min, the sample did not become fully isotropic at 260 °C and continued heating led to rapid cross-linking. Thus, the rapid cross-linking reaction imposes an experimental limit on the determination of the isotropization temperature at long cure times. At a cure temperature of 200 °C, the vitrification point was reached at approximately 4 h. The data in Figure 2 and Table 2 are presented as a function of cure time, instead of extent of reaction, due to the complicated nature of the cure reaction discussed below. We have not been able to quantify the reactions that occur at each cure time and thus cannot relate specific changes in the molecular structure to the transition temperatures.

Thermal Analysis. The thermal behavior of the monomers in Table 1 was investigated by DSC. Both heating and cooling cycles were recorded. All transition temperatures determined by DSC were consistent with the microscopy observations described earlier. Typical DSC traces are shown in Figures 3 and 4 for compounds **1** and **9**. For compound **1**, a crystal−crystal transition was seen at 142 °C, followed by the prominent melting to an anisotropic nematic phase at 167 °C. This compound subsequently displayed a transition to an isotropic fluid at 222 °C upon further heating. In this particular experiment, the cooling cycle was begun

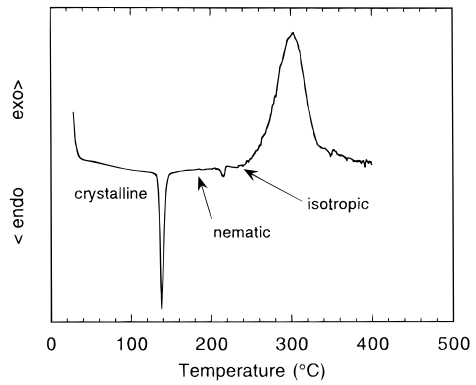

Figure 4. DSC heating curve including cross-linking exotherm for compound **9** recorded at 20 °C/min.

immediately after the isotropization transition and before significant reaction of the monomer. As seen in Figure 3, the transition to a nematic liquid crystalline phase occurred at virtually the same temperature as the isotropization transition on heating. Crystallization of the monomer occurred at 109 °C after significant (60 °C) supercooling of the nematic liquid.

The typical thermal behavior for a complete heating run is shown in Figure 4 for compound **9**. Transitions from a crystalline solid to a nematic liquid crystalline phase and from a nematic liquid crystalline phase to an isotropic liquid occurred at 134 and 211 °C, respectively. As was the case for all monomers studied, transition temperatures were unchanged when the maximum temperature attained during heating was maintained below the onset of cross-linking and the time scale of the experiment was relatively short. Further heating of compound **9** above the isotropization showed the onset of cross-linking at approximately 269 °C.

As seen in Table 1, the onset of cross-linking was consistently in the range 260−270 °C with peak maxima also consistently in the range 300−305 °C. Thus, the temperature for the onset of cross-linking appeared to be independent of the phase type since five of the monomers were in the nematic phase at these temperatures and the remainder of the monomers were in the isotropic phase. The DSC data were also used to calculate the transition entropies. For the compounds shown in Table 1, the range of values for the crystalline−liquid crystalline or crystalline−isotropic transitions was 0.044−0.070 cal/(g·K). There were not any particular trends evident that could be related to the molecular structures. However, the data could be grouped into two distinct categories. For those compounds that melted into a nematic phase, the transition entropies were less than 0.060 cal/(g·K). For the compounds that melted directly to the completely disordered isotropic liquid upon heating, the transition entropies were generally greater than 0.060 cal/(g·K). This is consistent with the expectation that the entropy change for a transition from a crystalline solid to an isotropic liquid would be larger than the entropy change for a transition from a crystalline solid to a partially ordered nematic phase.

Curing Behavior. It is generally accepted that the thermally induced cure reaction for propargyl thermosets is a rearrangement to a chromene ring, followed by step polymerization of the chromene[13−16] as il-

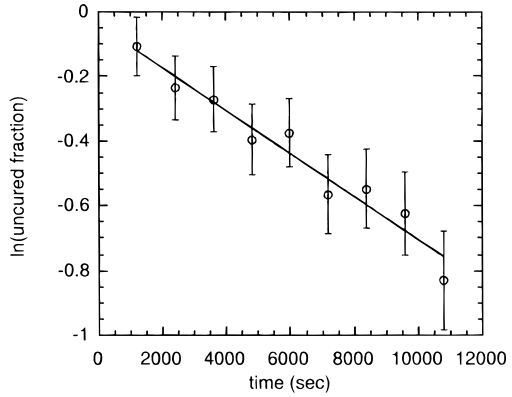

Figure 5. First-order kinetic plot for monomer **1** at 215 °C determined by DSC measurements.

lustrated in Figure 1b. This two-step reaction has been used to advantage in several cases; propargyl thermosets have been heated in the presence of various catalysts to create chromene-terminated resins with improved processing characteristics compared to the original propargyl-terminated resins.[16,30] A previous study has investigated the curing mechanism and kinetics for propargyl thermosets in some detail. Using ^{1}H and ^{13}C NMR, FTIR, and DSC, Grenier-Loustalot and Sanglar showed that formation of the chromene ring is more exothermic and has a lower rate constant than the subsequent polymerization of the chromene ring.[16] For our materials, the molecular weights of the samples cured at the various times were monitored by inherent viscosity measurements, performed at a concentration of 0.35% (w/v) in 1,1,2,2-tetrachloroethane at 30 °C. However, very little difference was seen in the samples cured at 0.5, 1.0, and 1.5 h, with all samples having an inherent viscosity of approximately 0.05 dL/g. This result is consistent with a two-step reaction in which chromene formation occurs very slowly and is the rate-limiting step.

Further support for the two-step mechanism comes from DSC measurements of the cure exotherm in the propargyl LCTs. Measurements of the cure exotherm for uncured samples of monomers **1** and **5** gave values of 422 ± 26 and 424 ± 28 kJ/mol, respectively. We have calculated a theoretical value for the cure exotherm based on bond energies. The calculation takes the first step of the reaction to be two carbon−carbon triple bonds per molecule breaking to form two double bonds and two single bonds, and the second step to be two carbon−carbon double bonds breaking to form four single bonds. Using standard values for the bond energies,[31] we obtain a theoretical cure exotherm of 403.4 kJ/mol. The agreement between this value and the experimental values provides additional confirmation that the cure of our LCTs occurs by the same mechanism as non-liquid-crystalline bispropargyl thermosets.

Detailed kinetic studies of the curing reaction were carried out by using DSC. The cure exotherms for partially cured samples were normalized to the cure exotherm for an uncured sample in order to determine the fraction of uncured sample remaining. Figure 5 shows a typical result of a first-order kinetic plot. Results are the same for monomer **1** at other temperatures up to 260 °C, as well as for monomer **5** at all temperatures from 215 to 260 °C. The first reaction step, chromene formation, is an intramolecular reaction and thus is expected to be first order. On the other hand, the second step, an ene−ene step polymerization reaction similar to indene polymerization,[32] should behave as a second-order reaction. An analysis of the kinetic data using second-order kinetics resulted in considerably poorer fits than shown in Figure 5. Although we cannot specifically separate out the amount of exotherm due to each reaction, this result supports the previous conclusion that the chromene formation is more exothermic than polymerization.[16] Thus, we can conclude that the cure exotherm, and our kinetic data, is dominated by the chromene formation, at least at the early stages of the reaction.

Table 3. First-Order Rate Constants for Monomers 1 and 5

temperature (°C)	k_1, monomer **1** (10^5 s^{-1})	k_1, monomer **5** (10^5 s^{-1})
215	6.6 ± 1.2	7.8 ± 0.9
230	17 ± 2	19 ± 4
245	43 ± 10	46 ± 5
260	89 ± 14	95 ± 15

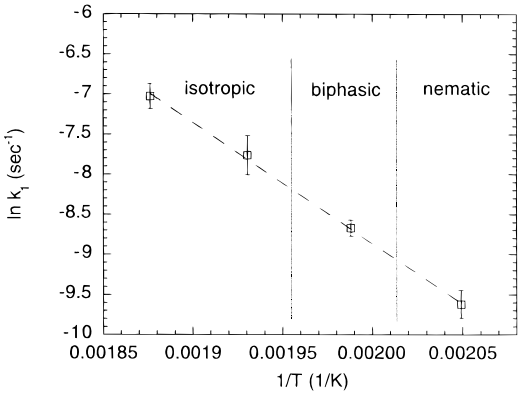

Figure 6. Arrhenius plot for the cure of monomer **1** based on the first-order rate constants. Temperature range 215−260 °C. The phase in which the cure takes place at each temperature is also indicated.

The first-order rate constants determined from the kinetic plots are given in Table 3. Within experimental error, there is no difference in the rate constants for the two monomers studied. Figure 6 shows the Arrhenius plot for monomer **1**. For convenience, the phases in which the reaction is taking place are also indicated in Figure 6. The activation energies determined from the Arrhenius plots are 125 ± 6 kJ/mol for monomer **1** and 120 ± 4 kJ/mol for monomer **5**.

The data in Table 3 and Figure 6 show no effect on the reaction rate due to the phase in which the reaction takes place. This is indicated in two ways. First, Table 3 shows no difference in the rate constants between the two monomers, although monomer **5** is isotropic at all temperatures, and monomer **1** is nematic at 215 °C, biphasic at 230 °C, and isotropic at the higher temperatures. Second, the Arrhenius plot in Figure 6 is linear;

(30) Godschalx, J. P.; Inbasekaran, M. N.; Bartos, B. R.; Scheck, D. M.; Laman, S. A. *SAMPE Technol. Conf.* **1990**, *22*, 163.
(31) Kemp, D. S.; Vellaccio, F. *Organic Chemistry*; Worth Publishers: New York, 1980; p 1058.
(32) Whitby, G. S.; Katz, M. *J. Am. Chem. Soc.* **1928**, *50*, 1160.

if there were a rate enhancement we would expect to see an upward curvature in the plot at high values of $1/T$.

Several studies have shown a clear rate enhancement for reactions that occur in liquid crystalline phases.[8,33,34] Recent reports from Bowman[35] and from Hoyle[36] have shown that the increase in the overall polymerization rate was due to a decrease in the termination rate constant in the liquid crystalline phase, while the propagation rate constant was essentially unchanged. The termination rate constant decreased due to changes in the diffusion of two reacting species toward each other in a bimolecular termination reaction. In both cases, the polymerizations conducted in these studies were chain growth polymerizations. Since the polymerization reaction of the intermediate chromene ring is a step growth reaction, similar discussions concerning changes in the termination rates are inapplicable. However, the present results are in good agreement with previous work on propargyl- and chromene-terminated prepolymers.[16] Overall, the polymerization of dipropargyl monomers can be viewed as two successive reactions, intramolecular ring formation and chromene polymerization. The previous authors[16] have shown that the rate constants for the polymerization of dipropargyl monomers are lower than those for dichromene monomers. The data and analysis presented here have demonstrated that the observed kinetics for the polymerization of dipropargyl monomers is first-order. Thus, we conclude that the overall observed reaction rate for the polymerization of dipropargyl monomers to polymer is controlled by the slow, rate-determining first step of chromene ring formation. This is expected to dominate the observed reaction kinetics at early reaction times. This is also consistent with the low inherent viscosities observed for the B-staged materials in this study.

Conclusions

We have synthesized a series of rigid-rod bispropargyl thermoset monomers based on aromatic ester rigid cores. Molecular structure effects were investigated by extending the length of the rigid core or by placing lateral substituents on the central core. Enantiotropic or monotropic nematic liquid crystalline phases were observed for most of the monomers. A monomer that did not originally display any liquid crystallinity was found to form a stable nematic phase after partial curing. Similarly, monomers that were initially monotropic formed broad enantiotropic nematic phases after partial curing. Only in the case of a bulky phenyl-substituted monomer was the complete absence of liquid crystalline phases noted. The phase behavior during curing was explained by the reactive nature of these materials, which leads to a combination of chain extension and network formation. We were able to experimentally verify many aspects of a transformation diagram that was previously proposed to explain the behavior of liquid crystalline thermosets. DSC investigations confirmed many of the microscopy observations. Additionally, the data indicated that the onset of thermally induced cross-linking was independent of the phase type, as some of the materials were in the isotropic phase while others were in the nematic phase at this temperature. Reaction rates were unaffected by the ordered liquid crystalline phase due to the intramolecular rearrangement to a chromene ring that dominates the cure reaction at early times.

Our future work will be directed at novel processing techniques and mechanical property evaluations of these and other new liquid crystalline thermosets. Our preliminary work in this area has already demonstrated significant enhancement of the mechanical properties of liquid crystalline thermosets as compared to conventional thermoset materials.[37]

Acknowledgment. This work was supported by Laboratory Directed Research and Development Funding of the Los Alamos National Laboratory, which is supported by the U.S. Department of Energy under Contract W-7405-ENG-36 to the University of California. E.D. acknowledges the donors of The Petroleum Research Fund, administered by the American Chemical Society, for partial support of this research. This material is based upon work supported in part by the U.S. Army Research Office under Grant DAAG55-98-1-0114 to E.D. as a Presidential Early Career Award for Scientists and Engineers.

CM980087B

(33) Hoyle, C. E.; Kang, D.; Chawla, C. P.; Griffin, A. C. *Polym. Eng. Sci.* **1992**, *32*, 1490.
(34) Hoyle, C. E.; Chawla, C. P.; Kang, D.; Griffin, A. C. *Macromolecules* **1993**, *26*, 758.
(35) Guymon, C. A.; Bowman, C. N. *Polym. Mater. Sci. Eng.* **1996**, *75*, 119.
(36) Williamson, S. E.; Kang, D.; Hoyle, C. E. *Macromolecules* **1996**, *29*, 8656.
(37) Smith, M. E.; Benicewicz, B. C.; Douglas, E. P.; Earls, J. D.; Priester, R. D., Jr. *Polym. Prepr.* **1996**, *37* (1), 50.